

Extract Propane and Ethane from Methane on Ultramicroporous Carbon Adsorbent with Record Selectivity

Fuqiang Chen¹, Kaiqing Guo¹, Xinlei Huang¹, Zhiguo Zhang¹, Qiwei Yang¹, Yiwen Yang¹, Qilong Ren¹, and Zongbi Bao¹

¹Zhejiang University

March 31, 2022

Abstract

Separation of light hydrocarbon mixtures and extraction of C₃H₈ and C₂H₆ from CH₄ are of significant importance in natural gas purification and upgrade. Microporous carbon adsorbents are promising in light hydrocarbons separation, but to fabricate uniform ultramicropores to boost separation selectivity remains challenging. Herein, we fabricated a series of poly(vinylidene chloride) resins-derived ultramicroporous carbon adsorbents with relatively uniform pore size (5.2-5.3 Å) by activator-free pyrolysis. The optimal C-PVDC-800 exhibited record-high IAST selectivity of C₃H₈/CH₄ (3387) and C₂H₆/CH₄ (75) as well as Henry's selectivity of C₃H₈/CH₄ (369) among all reported adsorbents under ambient conditions, combined with ultrahigh uptake of C₃H₈ (3.9 mmol g⁻¹, 0.05 bar) and C₂H₆ (2.67 mmol g⁻¹, 0.10 bar) at low partial pressures and 298 K. More importantly, fast gas adsorption kinetics were realized, favorable in fixed-bed adsorption applications. Breakthrough experiments and cycling tests further confirm the superb separation performance of extraction of C₃H₈ and C₂H₆ from CH₄.

Extract Propane and Ethane from Methane on Ultramicroporous Carbon Adsorbent with Record Selectivity

Fuqiang Chen^{1, #} | Kaiqing Guo^{1,3, #} | Xinlei Huang¹ | Zhiguo Zhang^{1,2} | Qiwei Yang^{1,2} | Yiwen Yang^{1,2} | Qilong Ren^{1,2} | and Zongbi Bao^{1,2, *}

¹Key Laboratory of Biomass Chemical Engineering of Ministry of Education,

College of Chemical and Biological Engineering, Zhejiang University, 38 Zheda Road, Hangzhou 310027, P. R. China

²Institute of Zhejiang University-Quzhou, 78 Jiuhua Boulevard North, Quzhou 324000, P. R. China

³Hangzhou Oxygen Plant Group Co., Ltd, Hangzhou 310014, P. R. China

#Co-authors: contributed equally to this work

*Corresponding authors: baozb@zju.edu.cn

Abstract

Separation of light hydrocarbon mixtures and extraction of C₃H₈ and C₂H₆ from CH₄ are of significant importance in natural gas purification and upgrade. Microporous carbon adsorbents are promising in light hydrocarbons separation, but to fabricate uniform ultramicropores to boost separation selectivity remains challenging. Herein, we fabricated a series of poly(vinylidene chloride) resins-derived ultramicroporous carbon adsorbents with relatively uniform pore size (5.2-5.3 Å) by activator-free pyrolysis. The optimal C-PVDC-800 exhibited record-high IAST selectivity of C₃H₈/CH₄ (3387) and C₂H₆/CH₄ (75) as well as Henry's selectivity of C₃H₈/CH₄ (369) among all reported adsorbents under ambient conditions, combined with ultrahigh uptake

of C_3H_8 (3.9 mmol g^{-1} , 0.05 bar) and C_2H_6 (2.67 mmol g^{-1} , 0.10 bar) at low partial pressures and 298 K. More importantly, fast gas adsorption kinetics were realized, favorable in fixed-bed adsorption applications. Breakthrough experiments and cycling tests further confirm the superb separation performance of extraction of C_3H_8 and C_2H_6 from CH_4 .

Keywords : microporous carbon adsorbents, light hydrocarbon, adsorption separation, natural gas purification

Introduction

Natural gas, mainly composed of methane, is regarded as an alternative energy source to traditional fossil fuels owing to abundant natural reserves and reduced pollutant emissions.¹⁻⁵ However, some other light hydrocarbons such as ethane and propane with the proportion of 12-39% also existed in natural gas, resulting in a reduced conversion rate as well as causing high risks in transportation.⁶⁻¹¹ Moreover, ethane and propane are essential fundamental feedstocks for the manufacture of vast varieties of basic chemicals.¹²⁻¹⁴ Consequently, separation of light hydrocarbons and extract C_3H_8 and C_2H_6 from CH_4 are not only beneficial in natural gas upgrading but also can obtain high value-added byproducts, remaining one of the critical processes in petrochemistry industry. Currently, the separation of light hydrocarbon mixtures mainly relies on cryogenic distillation, which is limited by huge energy input and harsh operation conditions.¹⁵ As a result, it is urgent to develop cost-effective and energy-saving technology. Adsorption separation process based on porous adsorbents has emerged as a promising alternative technology owing to high energy efficiency and mild operation conditions.¹⁶⁻²⁴

In recent decades, numerous varieties of porous adsorbents such as metal-organic frameworks (MOFs)^{9,10,25-29}, zeolites^{12,30-32} and porous carbon adsorbents³³⁻³⁵ have been intensively investigated for light hydrocarbon separations. MOFs with tunable surface chemistry and well-dedicated pore structure have made great process in light hydrocarbon separations, but the stability and expensive manufacture cost make them less attractive in practical applications. Moreover, strong affinities towards gas molecules arouse from strongly polarized pore channel of zeolites make regeneration a harsh process.²⁰ In contrast, porous carbons are considered as promising adsorbents for applications in harsh industrial conditions, benefiting from robust stability, low fabrication cost and water resistance.^{3,36-38}

Traditional carbon adsorbents are mainly fabricated by chemical activation method,³⁹⁻⁴¹ which possess high surface areas and exhibited high uptake of light hydrocarbons. For instance, Zhang et al. reported a group of algae-derived porous carbon adsorbents with ultrahigh surface areas ($> 1400 \text{ m}^2\text{g}^{-1}$) via chemical activation.⁴² And high uptake of C_3H_8 (11.5 mmol g^{-1}) and C_2H_6 (6.84 mmol g^{-1}) were achieved on the ANPC sample at 1 bar and 298 K. Nevertheless, the wide pore size distributions of these carbon adsorbents make it difficult to discriminate gas molecules via dimensional difference, thus resulting in poor selectivity of $\text{C}_3\text{H}_8/\text{CH}_4$ (189) and $\text{C}_2\text{H}_6/\text{CH}_4$ (15.3). To this end, nitrogen-doped hierarchical porous carbons were prepared by Deng's group.⁴³ A narrow pore size distribution (2.6-3.2 nm) was obtained, and the optimal NACs exhibited excellent uptake of hydrocarbons (C_2H_6 : 7.59 mmol g^{-1} , C_3H_8 : $11.77 \text{ mmol g}^{-1}$) combined with high selectivity of $\text{C}_3\text{H}_8/\text{CH}_4$ (501.9) and $\text{C}_2\text{H}_6/\text{CH}_4$ (65.7). Nonetheless, the cumbersome fabrication process including pre-polymerization, carbonization and acid washing make it urgent to explore a facile strategy for preparing microporous carbon adsorbents with excellent separation performance of light hydrocarbons. Accordingly, Lu et al. reported a thermo-regulated phase transition strategy for the fabrication of 2D flat carbon nanoplates with uniform ultramicropores (5.6 Å).³⁵ Thanks to the uniform pore size and large pore volume, ultrahigh uptake of C_3H_8 (3.36 mmol g^{-1} at 0.05 bar) and C_2H_6 (3.8 mmol g^{-1} at 0.10 bar) at low partial pressures and 298 K were achieved, further demonstrating the crucial role of micropore in hydrocarbons adsorption.

Besides pore size and preparation method, particle size of carbon adsorbents is also important. Generally, the utilization of adsorbents in powder may encounter many problems such as pipe blockage and pressure drop throughout fixed-bed,⁴⁴ posing strict requirements on shaping adsorbents. With these considerations in mind, monodispersed poly(vinylidene chloride) (PVDC) resins with large particle size were served as precursor to fabricate a series of microporous carbon adsorbents via one-step activation agent-free pyrolysis.

These PVDC-derived carbon adsorbents exhibited uniform spherical morphology with the particle size of 100-200 μm , which is suitable for being packed in fixed-bed. Moreover, the spontaneous release of hydrogen chloride molecules generated a well-developed microporous structure, and ultrahigh surface areas ($> 1000 \text{ m}^2 \text{ g}^{-1}$) and pore volume ($> 0.37 \text{ cm}^3 \text{ g}^{-1}$) were achieved. Motivated by the well-developed porosity and uniform morphology, adsorption tests of light hydrocarbons including C_3H_8 , C_2H_6 and CH_4 were performed. As expected, ultrahigh uptake of C_3H_8 (3.90 mmol g^{-1} at 0.10 bar) and C_2H_6 (2.67 mmol g^{-1} at 0.05 bar) at low partial pressures and 298 K were achieved on the optimal C-PVDC-800. Remarkably, the IAST selectivity of $\text{C}_3\text{H}_8/\text{CH}_4$ (50/50, v/v) and $\text{C}_2\text{H}_6/\text{CH}_4$ (50/50, v/v) at 298 K and 100 kPa was calculated to be 3387 and 75, respectively, outperforming all reported adsorbents. As well, the fast adsorption kinetics of light hydrocarbons on the carbon adsorbent were also confirmed. Breakthrough experiments further verify the superb separation performance of the mixtures of light hydrocarbons.

Experimental section

Materials

Poly(vinylidene chloride) resins were acquired from Juhua Group Co., Ltd. (China). High purity C_3H_8 ($>99.99\%$), C_2H_6 ($>99.99\%$), CH_4 ($>99.995\%$), He (99.999%) and N_2 ($>99.999\%$) were obtained from Jingong Co., Ltd. (China). Gas mixtures of $\text{C}_3\text{H}_8/\text{CH}_4$ (50/50), $\text{C}_2\text{H}_6/\text{CH}_4$ (50/50, v/v) and $\text{C}_3\text{H}_8/\text{C}_2\text{H}_6/\text{CH}_4$ (5/10/85, v/v/v) were bought from Weichuang Standard Gas Analysis Technology Co., Ltd. (China).

Preparation process

The synthesis of PVDC-derived carbon adsorbents was carried out based on our previously reported method.³ PVDC resins, placed into tube furnace, were directly heated to the temperature of 600-900 under a high-purity nitrogen atmosphere with a flow rate of 25 mL min^{-1} and cooled naturally. The heating rate before 500 is 1 min^{-1} , and the heating rate changed to 5 min^{-1} after 500. The prepared carbon adsorbents were named as C-PVDC-T, and T indicates the ultimate pyrolysis temperatures.

Characterization

Powder X-ray diffraction (PXRD) patterns of these carbon adsorbents were obtained on a X'Pert diffractometer (Panalytical Corp., Netherlands) using Cu $\text{K}\alpha$ radiation ($\lambda = 1.542 \text{ \AA}$) with 0.02° steps in the $5\text{-}80^\circ$ angular range. Scanning electron microscope (SEM) was performed at a Hitachi SU-70 (Hitachi Corp. Japan). Raman spectroscopy was conducted on LabRAM HR Evolution (Thermo Fischer, USA). X-ray photoelectron spectroscopy (XPS) was measured on a Thermo ESCALAB 250Xi spectrometer provided with a monochromated Al $\text{K}\alpha$ X-ray source ($h\nu = 1486.6 \text{ eV}$, 15 kV, 10.8 mA). A criterion of C_{1s} peak (284.8 eV) was used as a reference in calibrating the binding energy. Brunauer-Emmett-Teller (BET) specific surface areas and pore size distributions were examined by N_2 adsorption-desorption isotherms at 77 K, which were performed on Micromeritics ASAP 2020 Plus HD88. Thermogravimetric analysis of the samples were conducted on a Pyris1 TGA instrument (Perkin-Elmer Corp.) from 50-900 with a heating rate of 10 min^{-1} in N_2 atmosphere. Elemental analysis was carried out on a Elenmetar Analysensysteme GmbH.

2.4 Static adsorption tests

Single-component adsorption isotherms of C_3H_8 , C_2H_6 and CH_4 at 298 K and 273 K were collected on volumetric adsorption analyzer (Micromeritics 3Flex). About 100 mg of carbon adsorbents were utilized for gas sorption tests. Before gas adsorption measurements, the degas process was carried out under vacuum at 150°C for 12 h. The free space was determined by using helium.

2.5 Kinetic adsorption tests

The kinetic adsorption profiles were collected on the Intelligent Gravimetric Analyzer (IGA001, Hiden, UK), which uses a gravimetric technique to record the transient gas uptake as a function of time under various operating conditions. In each test, about 40 mg of carbon adsorbents was loaded into the sample basket, and then the system was outgassed at 423 K for 12 h before the dynamic gas adsorption tests. The adsorption

kinetics were obtained by measuring mass change at 1000 mbar at 298 K, and the pressure was boosted up by introducing the target gas into the sample chamber from 0 mbar to 1000 mbar at 200 mbar min⁻¹. After each test, the chamber was backfilled with the target gas to 1000 mbar, and the sample was replaced by the new sample for the next test. All the gases used (C₃H₈, C₂H₆ and CH₄) were of high purity (>99.99%).

Breakthrough experiments

Typically, a certain amount of C-PVDC-800 (1.0 g) was degassed prior to being packed into a stainless steel HPLC column (4.6 mm I.D. × 100 mm). The package of the column was carried out in glovebox filled with argon. A flow of helium was introduced into the column to further purge the sample before performing breakthrough experiments. Then the column was purged under the flowing helium at 150 °C for 24 h. In the breakthrough experiments, the gas mixtures of C₃H₈/CH₄ (50/50, v/v), C₂H₆/CH₄ (50/50, v/v) and C₃H₈/C₂H₆/CH₄ (5/10/85, v/v/v) were injected with a flow rate of 2.0 mL min⁻¹. The outlet gas of the column was detected by GC-2010 Plus gas chromatography (Shimadzu, Japan) with a flame ionization detector. After every breakthrough measurement, the packing column was regenerated with a He flow (20 mL min⁻¹) at 150 °C for 24 h, and then the repeated breakthrough tests were performed under the identical conditions.

3 Results and Discussion

3.1 Structure characterization

A series of PVDC resins derived carbon adsorbents were successfully synthesized according to our previously reported literature.³ The prepared carbon adsorbents remained the spherical morphology with slightly reduced particles size ranging from 100-200 μm compared with the precursor (Figure 1a and Figure S1), and the rough surfaces of the carbon adsorbent were caused by the formation of abundant micropores. As displayed in Figure 1a, these carbon adsorbents exhibited the typical characteristics of amorphous structure, with two wide peaks concentrated at 25° and 43°, corresponding to the (002) and (101) plane, respectively. The degree of structure defects was also determined by Raman spectra (Figure 1c), all these carbon adsorbents exhibited abundant structure defects with the I_D/I_G values calculated to be large than 2.0 (Table S1). It can be observed that the I_D/I_G value decreased with the increases of pyrolysis temperature, which may be caused by the enhanced graphitization at higher carbonization temperature. The chemical compositions of these carbon surfaces were investigated by XPS spectra. And no distinct peaks of Cl_{2p} are present, indicating no residues of chlorine element in the carbon skeleton. Moreover, verified by the deconvolution of high-resolution C_{1s} spectrum, abundant oxygen-containing functional groups (C-C, C-O-C, C=O and O-C=O) can be observed (Figure 1d, Figure S2), which may be favorable for light hydrocarbons adsorption. N₂ adsorption tests at 77 K were performed to investigate the porous structure of these carbon adsorbents (Figure S3). The BET specific areas were calculated to be 1087-1365 m² g⁻¹, and large pore volumes (0.38-0.47 cm³ g⁻¹) were also achieved (Table S2). Notably, unimodal pore size distributions were obtained, with the median pore size concentrated at 5.2 to 5.3 Å for C-PVDC-T. The pore sizes comparable to the kinetic diameter of C₃H₈ (5.1 Å) enhance the micropore confinement effect of the gas molecules. All the characterization results matches well with our previous work³, and the minor numeric differences may be caused by the parameters (eg. temperature, flow rate, etc.) fluctuations during different batches of pyrolysis and deviation of testing instruments.

3.2 Adsorption tests

Inspired by the well-developed porosity and appropriate pore sizes, the adsorption isotherms of C₃H₈, C₂H₆ and CH₄ at 273 K and 298 K were collected (Figure 2a-b, Figure S4-5). As expected, these carbon adsorbents exhibited the steeply rising isotherms of C₃H₈ and C₂H₆, while the isotherms of CH₄ is quite gentle. The C-PVDC-800 possessed the highest uptake of C₃H₈ (5.21 mmol g⁻¹) and C₂H₆ (5.28 mmol g⁻¹) at 298 K and 1.0 bar than other carbon adsorbents. Remarkably, 6.9 C₂H₆ and 7.0 C₃H₈ molecules per nm³pore volume can be captured by C-PVDC-800, indicating a dense packing of light hydrocarbons in the pore structure. Noticeably, these carbon adsorbent still hold high uptake of C₃H₈ and C₂H₆ at low pressure range (< 0.1 bar) combined with a negligible uptake of CH₄, thus resulting in high selectivity of C₃H₈/CH₄ and C₂H₆/CH₄

(Figure 2c, Figure S6). Specifically, the uptake of C_3H_8 on C-PVDC-800 at 0.05 bar and 298 K was measured to be 3.90 mmol g^{-1} , surpassing most reported adsorbents such as FCP-1-KC (3.80 mmol g^{-1})³⁵, A-AC-4 (3.74 mmol g^{-1})⁴⁵, JLU-Liu7 (3.08 mmol g^{-1})⁴⁶, MFM-202a (1.73 mmol g^{-1})²⁸ and BSF-1 (1.23 mmol g^{-1})²⁶, only next to NAC-700 (4.78 mmol g^{-1})³³ (Figure 2d, Table S7). The uptake of C_2H_6 on C-PVDC-800 at 0.10 bar and 298 K was 2.67 mmol g^{-1} , also outperforming most adsorbents like FJI-C4 (2.65 mmol g^{-1})¹⁰, NAHA-2 (2.2 mmol g^{-1})³⁴, NAC-700 (2.06 mmol g^{-1})³³ and JLU-Liu15 (1.70 mmol g^{-1})⁴⁷, only next to the benchmark carbon adsorbent FCP-1-KC (3.36 mmol g^{-1})²⁶ (Figure 2e, Table S7). The IAST selectivity of C_3H_8/CH_4 (50/50, v/v) and C_2H_6/CH_4 (50/50, v/v) was calculated to estimate the separation potential (Figure S6, Table S7). Surprisingly, record high IAST selectivity of C_3H_8/CH_4 (3387) and C_2H_6/CH_4 (75) at 298 K and 100 kPa was achieved on C-PVDC-800, which set a new benchmark for light hydrocarbons separation. Additionally, Henry's selectivity of C_3H_8/CH_4 was also calculated by fitting isotherms in low-pressure range (Figure 2f, Table S8-9). Compared with other materials, C-PVDC-800 exhibited the record high Henry's selectivity of C_3H_8/CH_4 (369), demonstrating the great potential of extraction of C_3H_8 with low concentration from CH_4 . The heat of adsorption (Q_{st}) curves of C_3H_8 , C_2H_6 and CH_4 were obtained according to viral method (Figure S7, Table S10-12). The Q_{st} at zero-coverage of C_3H_8 , C_2H_6 and CH_4 on C-PVDC-800 were calculated to be 78.1, 35.6 and 19.5 kJ mol^{-1} , respectively. The Q_{st} on other carbon adsorbents also followed the order: $C_3H_8 > C_2H_6 > CH_4$, indicating the strength of adsorption affinities toward different gas molecules.

3.3 Kinetic adsorption tests

Adsorption kinetics reflect the diffusion rate of gas molecules in porous adsorbent, which is vital in determining efficiency in practical separation process. Time-dependent adsorption isotherms of C_3H_8 , C_2H_6 and CH_4 on C-PVDC-800 at 100 kPa and 298 K were performed (Figure 3a). The time of adsorption for C_3H_8 , C_2H_6 and CH_4 to reach equilibrium at 298 K and 100 kPa was measured to be 5.0, 5.3 and 5.4 min, respectively. The equilibrium adsorption uptake of C_3H_8 , C_2H_6 and CH_4 reached up to 5.17, 5.29 and 1.54 mmol g^{-1} , respectively, consistent with the results obtained from the static adsorption tests. Based on the classic micropore diffusion mode⁴⁸, the micropore diffusion time constants of C_3H_8 , C_2H_6 and CH_4 were calculated to be 2.73×10^{-2} , 1.69×10^{-2} and $1.18 \times 10^{-2} \text{ min}^{-1}$, respectively (Figure 3c). Notably, the diffusion time constants of these hydrocarbon molecules follow the order: $C_3H_8 > C_2H_6 > CH_4$, since the effective diffusion coefficient was governed by a combination of molecular kinetic properties and adsorption thermodynamics.^{49,50} Based on Costa's proposal⁴⁸, the internal diffusion coefficient (D_i) can be described by the equation:

$$D_i = D_g + KD_s \quad (1)$$

Where D_g represents the Knudsen diffusion coefficient, K is proportional to the slope of the equilibrium isotherms, D_s represents the surface migration coefficient. Moreover, the contribution of KD_s to the total D_i reaches up to 70-80%. Since the pore size of the carbon adsorbent is larger than these guest molecules, under such circumstance, there is no distinct difference in D_g and D_s of these hydrocarbon molecules. As noted by the adsorption isotherms (Figure 2a), the slope of C_3H_8 is the steepest, followed by C_2H_6 and CH_4 successively, leading to a decreasing trend in K . Consequently, the faster diffusion coefficient with the increasing of carbon number of gas molecules can be obtained. In general, fast adsorption kinetics of these hydrocarbon molecules indicate the ultramicropores in C-PVDC-800 are easily accessible, offering great potential in practical separation process.

3.4 Breakthrough experiments and stability

To verify the separation potential for hydrocarbon mixtures, breakthrough experiments were conducted. As for C_3H_8/CH_4 (50/50, v/v) mixture, complete separation of C_3H_8 and CH_4 was realized on C-PVDC-800 (Figure 4a). CH_4 eluted at 20 min, while the breakthrough time of C_3H_8 (90 min) was quite longer, thus obtaining a high-purity CH_4 ($> 99.9\%$) with productivity reaching up to 5.23 mmol g^{-1} . And the dynamic adsorption uptake of C_3H_8 was calculated to be 4.07 mmol g^{-1} , slightly lower than the pure C_3H_8 adsorption data at partial pressure of 50 kPa. Similarly, C-PVDC-800 also realized an excellent separation performance of C_2H_6/CH_4 (50/50, v/v) mixture (Figure 4b). CH_4 first escaped from the adsorption column with the

breakthrough time of 20 min, and C_2H_6 was subsequently detected until 80 min. The dynamic adsorption uptake of C_2H_6 and high-purity productivity of CH_4 were calculated to be 3.63 mol g^{-1} and 4.57 mmol g^{-1} , respectively. To predict the performance of practical natural gas purification, breakthrough experiments using ternary $C_3H_8/C_2H_6/CH_4$ (5/10/85, v/v/v) gas mixture were performed (Figure 4c). Consistent with the adsorption selectivity, CH_4 first broke through the column at 17 min, followed by C_2H_6 (205 min) and C_3H_8 (670 min) with longer breakthrough time. Obviously, the prepared C-PVDC-800 can separate the feed ternary gas mixtures into three individual purified components with a high productivity of high-purity CH_4 ($15.72 \text{ mmol g}^{-1}$). Detailed separation performance of various gas mixtures on C-PVDC-800 was outlined in Figure S13.

Moreover, cycling breakthrough experiments using ternary gas mixture were performed. As illustrated in Figure 4d, no apparent decay of breakthrough time of the gas molecules was observed after 5 cycles, reflecting excellent cycling stability and easy regeneration of the carbon adsorbent. As noted in Figure S8, there is no obvious weight loss of C-PVDC-800 was seen even at 900 °C under nitrogen atmosphere, demonstrating this carbon adsorbent is thermally stable under harsh industrial operation conditions. Chemical compositions of the carbon adsorbents were examined by elemental analysis (Table S14). All these carbon adsorbents exhibited a high carbon content, providing structure basis for the robust thermal and chemical stability. And the C/O ratio increased with the increase of pyrolysis temperature.

Conclusion

In summary, a group of ultramicroporous carbon adsorbents were successfully fabricated by activator-free pyrolysis strategy. Thanks to the well-developed porous structure and appropriate pore size, the optimal C-PVDC-800 exhibited record-high IAST selectivity of C_3H_8/CH_4 (3387) and C_2H_6/CH_4 (75) well as Henry's selectivity of C_3H_8/CH_4 (375) at 100 kPa and 298 K, combined with ultrahigh uptake of C_3H_8 (3.90 mmol g^{-1} at 0.10 bar) and C_2H_6 (2.67 mmol g^{-1} at 0.05 bar) at low partial pressures and 298 K. More importantly, fast adsorption kinetics of the hydrocarbon molecules were realized in this carbon adsorbent, offering great potential in practical applications. Breakthrough experiments further verify the superb separation performance of light hydrocarbon mixtures. High adsorption capacity, fast adsorption kinetics, facile preparation method and robust stability guarantee this carbon adsorbent highly promising in natural gas purification and the extraction of C_3H_8 and C_2H_6 from CH_4 . The synthesized ultramicroporous carbon adsorbents may also show great potential in other gas mixtures' separation.

Acknowledgements

This work was supported by the National Natural Science Foundation of China (No. 21878260, No. 21978254 and No. 22141001).

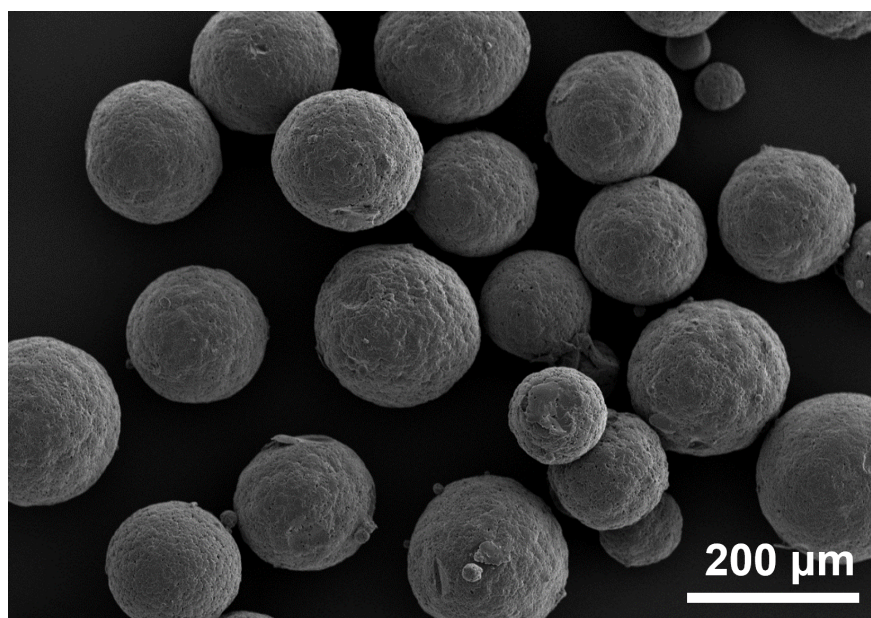
References

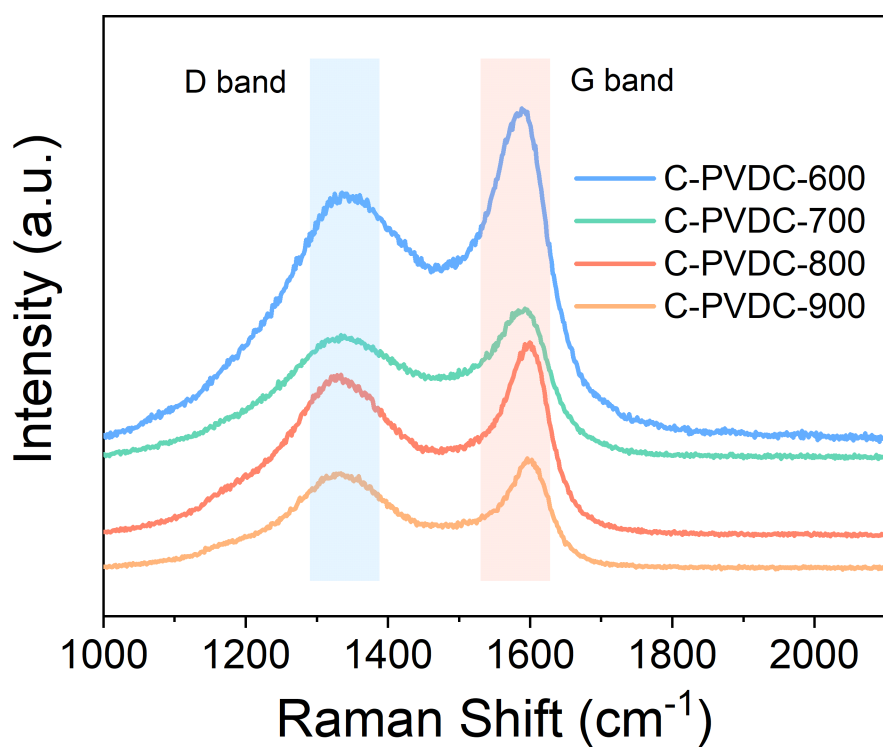
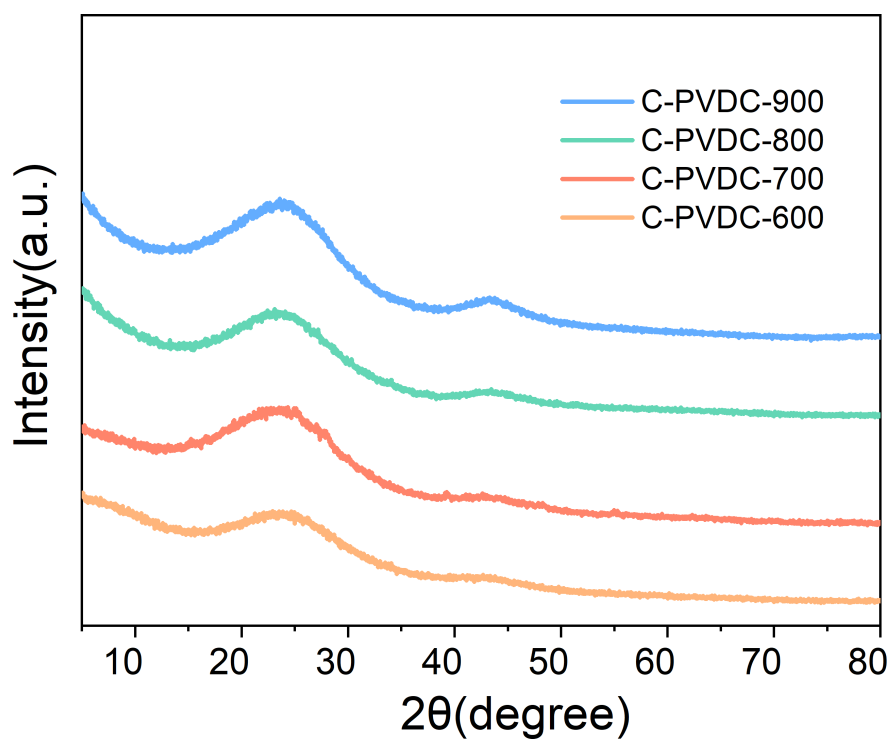
1. Connolly BM, Aragonés-Anglada M, Gandara-Loe J, et al. Tuning porosity in macroscopic monolithic metal-organic frameworks for exceptional natural gas storage. *Nat. Commun.* 2019;10:2345.
2. Saha D, Grappe HA, Chakraborty A, Orkoulas G. Postextraction Separation, On-Board Storage, and Catalytic Conversion of Methane in Natural Gas: A Review. *Chem. Rev.* 2016;116(19):11436-11499.
3. Chen FQ, Zhang ZG, Yang QW, Yang YW, Bao ZB, Ren QL. Microporous Carbon Adsorbents Prepared by Activating Reagent-Free Pyrolysis for Upgrading Low-Quality Natural Gas. *ACS Sustainable Chem. Eng.* 2020;8(2):977-985.
4. Lv D, Wu Y, Chen J, et al. Improving CH_4/N_2 selectivity within isomeric Al-based MOFs for the highly selective capture of coal-mine methane. *AIChE J.* 2020;66(9):e16287.
5. Hu G, Xiao G, Guo Y, et al. Separation of methane and nitrogen using ionic liquid zeolites (ILZ) by pressure vacuum swing adsorption (PVSA). *AIChE J.* 2022:e17668. doi:10.1002/aic.17668.

6. Shen JM, Dailly A, Beckner M. Natural gas sorption evaluation on microporous materials. *Micropor. Mesopor. Mat.* 2016;235:170-177.
7. Duan X, He Y, Cui Y, et al. Highly selective separation of small hydrocarbons and carbon dioxide in a metal-organic framework with open copper (II) coordination sites. *RSC Adv.* 2014;4(44):23058-23063.
8. Yao S, Wang DM, Cao Y, Li GH, Huo QS, Liu YL. Two stable 3D porous metal-organic frameworks with high performance for gas adsorption and separation. *J. Mater. Chem. A.* 2015;3(32):16627-16632.
9. Wang DM, Zhao TT, Cao Y, et al. High performance gas adsorption and separation of natural gas in two microporous metal-organic frameworks with ternary building units. *Chem. Commun.* -2014;50(63):8648-8650.
10. Li L, Wang XS, Liang J, et al. Water-Stable Anionic Metal-Organic Framework for Highly Selective Separation of Methane from Natural Gas and Pyrolysis Gas. *ACS Appl. Mater. Inter.* 2016;8(15):9777-9781.
11. Li JT, Luo XL, Zhao NA, Zhang LR, Huo QS, Liu YL. Two Finite Binuclear $[M_2(\mu_2-OH)(COO)_2]$ (M= Co, Ni) Based Highly Porous Metal-Organic Frameworks with High Performance for Gas Sorption and Separation. *Inorg. Chem.* 2017;56(7):4141-4147.
12. Perez LE, Avila AM, Sawada JA, Rajendran A, Kuznicki SM. Process optimization-based adsorbent selection for ethane recovery from residue gas. *Sep. Purif. Technol.* 2016;168:19-31.
13. Banerjee D, Liu J, Thallapally PK. Separation of C2 Hydrocarbons by Porous Materials: Metal Organic Frameworks as Platform. *Comments Inorg. Chem.* 2015;35(1):18-38.
14. Ren T, Patel M, Blok K. Olefins from conventional and heavy feedstocks: Energy use in steam cracking and alternative processes. *Energy.* 2006;31(4):425-451.
15. Sholl DS, Lively RP. Seven chemical separations to change the world. *Nature.* 2016;532(7600):435-437.
16. Bae YS, Snurr RQ. Development and evaluation of porous materials for carbon dioxide separation and capture. *Angew. Chem. Int. Ed.* 2011;50(49):11586-11596.
17. Cadiau A, Adil K, Bhatt PM, Belmabkhout Y, Eddaoudi M. A metal-organic framework-based splitter for separating propylene from propane. *Science.* 2016;353(6295):137-140.
18. Nugent P, Belmabkhout Y, Burd SD, et al. Porous materials with optimal adsorption thermodynamics and kinetics for CO₂ separation. *Nature.* 2013;495(7439):80-84.
19. Liao PQ, Huang NY, Zhang WX, Zhang JP, Chen XM. Controlling guest conformation for efficient purification of butadiene. *Science.* 2017;356(6343):1193-1196.
20. Chen FQ, Lai D, Guo LD, et al. Deep Desulfurization with Record SO₂ Adsorption on the Metal-Organic Frameworks. *J. Am. Chem. Soc.* 2021;143(26):9040-9047.
21. Zhao X, Wang Y, Li DS, Bu X, Feng P. Metal-organic frameworks for separation. *Adv. Mater.* 2018;30(37):1705189.
22. Lyndon R, You WQ, Ma Y, et al. Tuning the Structures of Metal-Organic Frameworks via a Mixed-Linker Strategy for Ethylene/Ethane Kinetic Separation. *Chem. Mater.* 2020;32(9):3715-3722.
23. Furukawa H, Cordova KE, O’Keeffe M, Yaghi OM. The chemistry and applications of metal-organic frameworks. *Science.* 2013;341(6149):1230444.
24. Hu Z, Wang Y, Wang X, Zhai L, Zhao D. Solution-reprocessable microporous polymeric adsorbents for carbon dioxide capture. *AIChE J.* 2018;64(9):3376-3389.
25. Yuan YN, Wu HX, Xu YZ, et al. Selective extraction of methane from C1/C2/C3 on moisture-resistant MIL-142A with interpenetrated networks. *Chem. Eng. J.* 2020;395.

26. Zhang YB, Yang LF, Wang LY, Duttwyler S, Xing HB. A Microporous Metal-Organic Framework Supramolecularly Assembled from a Cu-II Dodecaborate Cluster Complex for Selective Gas Separation. *Angew. Chem. Int. Ed.* 2019;58(24):8145-8150.
27. He YB, Zhang ZJ, Xiang SC, Fronczek FR, Krishna R, Chen BL. A robust doubly interpenetrated metal-organic framework constructed from a novel aromatic tricarboxylate for highly selective separation of small hydrocarbons. *Chem. Commun.* 2012;48(52):6493-6495.
28. Gao S, Morris CG, Lu ZZ, et al. Selective Hysteretic Sorption of Light Hydrocarbons in a Flexible Metal-Organic Framework Material. *Chem. Mater.* 2016;28(7):2331-2340.
29. Jia JT, Wang L, Sun FX, et al. The Adsorption and Simulated Separation of Light Hydrocarbons in Isorecticular Metal-Organic Frameworks Based on Dendritic Ligands with Different Aliphatic Side Chains. *Chem.-Eur. J.* 2014;20(29):9073-9080.
30. Peralta D, Chaplais G, Simon-Masseron A, et al. Comparison of the behavior of metal-organic frameworks and zeolites for hydrocarbon separations. *J. Am. Chem. Soc.* 2012;134(19):8115-8126.
31. Dong J, Lin Y, Liu W. Multicomponent hydrogen/hydrocarbon separation by MFI-type zeolite membranes. *AIChE J.* 2000;46(10):1957-1966.
32. Yang Y, Burke N, Ali S, Huang S, Lim S, Zhu Y. Experimental studies of hydrocarbon separation on zeolites, activated carbons and MOFs for applications in natural gas processing. *RSC Adv.* 2017;7(21):12629-12638.
33. Wang J, Krishna R, Yang T, Deng SG. Nitrogen-rich microporous carbons for highly selective separation of light hydrocarbons. *J. Mater. Chem. A*. 2016;4(36):13957-13966.
34. Yuan B, Wang J, Chen YX, Wu XF, Luo HM, Deng SG. Unprecedented performance of N-doped activated hydrothermal carbon towards C₂H₆/CH₄, CO₂/CH₄, and CO₂/H₂ separation. *J. Mater. Chem. A*. 2016;4(6):2263-2276.
35. Zhang LH, Li WC, Liu H, et al. Thermoregulated Phase-Transition Synthesis of Two-Dimensional Carbon Nanoplates Rich in sp² Carbon and Unimodal Ultramicropores for Kinetic Gas Separation. *Angew. Chem.* 2018;130(6):1648-1651.
36. Chen FQ, Ding JQ, Guo KQ, et al. CoNi Alloy Nanoparticles Embedded in Metal-Organic Framework-Derived Carbon for the Highly Efficient Separation of Xenon and Krypton via a Charge-Transfer Effect. *Angew. Chem. Int. Ed.* 2021;60(5):2431-2438.
37. Du SJ, Huang JW, Anjum AW, Xiao J, Li Z. A novel mechanism of controlling ultramicropore size in carbons at sub-angstrom level for molecular sieving of propylene/propane mixtures. *J. Mater. Chem. A*. 2021;9(42):23873-23881.
38. Saha D, Deng SG. Adsorption equilibrium and kinetics of CO₂, CH₄, N₂O, and NH₃ on ordered mesoporous carbon. *J. Colloid. Interf. Sci.* 2010;345(2):402-409.
39. Cai J, Qi J, Yang C, Zhao X. Poly (vinylidene chloride)-based carbon with ultrahigh microporosity and outstanding performance for CH₄ and H₂ storage and CO₂ capture. *ACS Appl. Mater. Inter.* 2014;6(5):3703-3711.
40. Yang X, Yu M, Zhao Y, Zhang C, Wang XY, Jiang JX. Remarkable gas adsorption by carbonized nitrogen-rich hypercrosslinked porous organic polymers. *J. Mater. Chem. A*. 2014;2(36):15139-15145.
41. Zhang Y, Zhang PX, Yu WK, et al. Facile and Controllable Preparation of Ultramicroporous Biomass-Derived Carbons and Application on Selective Adsorption of Gas-mixtures. *Ind. Eng. Chem. Res.* 2018;57(42):14191-14201.

42. Zhang PX, Wen X, Wang L, et al. Algae-derived N-doped porous carbons with ultrahigh specific surface area for highly selective separation of light hydrocarbons. *Chem. Eng. J.* 2020;381:122731.
43. Meng S, Ma HP, Jiang LC, Ren H, Zhu GS. A facile approach to prepare porphyrinic porous aromatic frameworks for small hydrocarbon separation. *J. Mater. Chem. A.* 2014;2(35):14536-14541.
44. Wu KY, Guo LD, Zhang ZG, et al. Shaping of gallate-based metal-organic frameworks for adsorption separation of ethylene from acetylene and ethane. *J. Colloid. Interf. Sci.* 2021;581:177-184.
45. Liang WW, Xiao HY, Lv DF, Xiao J, Li Z. Novel asphalt-based carbon adsorbents with super-high adsorption capacity and excellent selectivity for separation for light hydrocarbons. *Sep. Purif. Technol.* 2018;190:60-67.
46. Luo JH, Wang J, Cao Y, et al. Assembly of an indium-porphyrin framework JLU-Liu7: a mesoporous metal-organic framework with high gas adsorption and separation of light hydrocarbons. *Inorg. Chem. Front.* 2017;4(1):139-143.
47. Luo XL, Sun LB, Zhao J, et al. Three Metal-Organic Frameworks Based on Binodal Inorganic Building Units and Hetero-O, N Donor Ligand: Solvothermal Syntheses, Structures, and Gas Sorption Properties. *Cryst. Growth Des.* 2015;15(10):4901-4907.
48. Ruthven DM. *Principles of adsorption and adsorption processes*. New York: John Wiley & Sons, Inc., 1984.
49. Costa E, Calleja G, Domingo F. Adsorption of gaseous hydrocarbons on activated carbon: Characteristic kinetic curve. *AIChE J.* 1985;31(6):982-991.
50. Birkmann F, Pasel C, Luckas M, Bathen D. Adsorption thermodynamics and kinetics of light hydrocarbons on microporous activated carbon at low temperatures. *Ind. Eng. Chem. Res.* 2018;57(23):8023-8035.





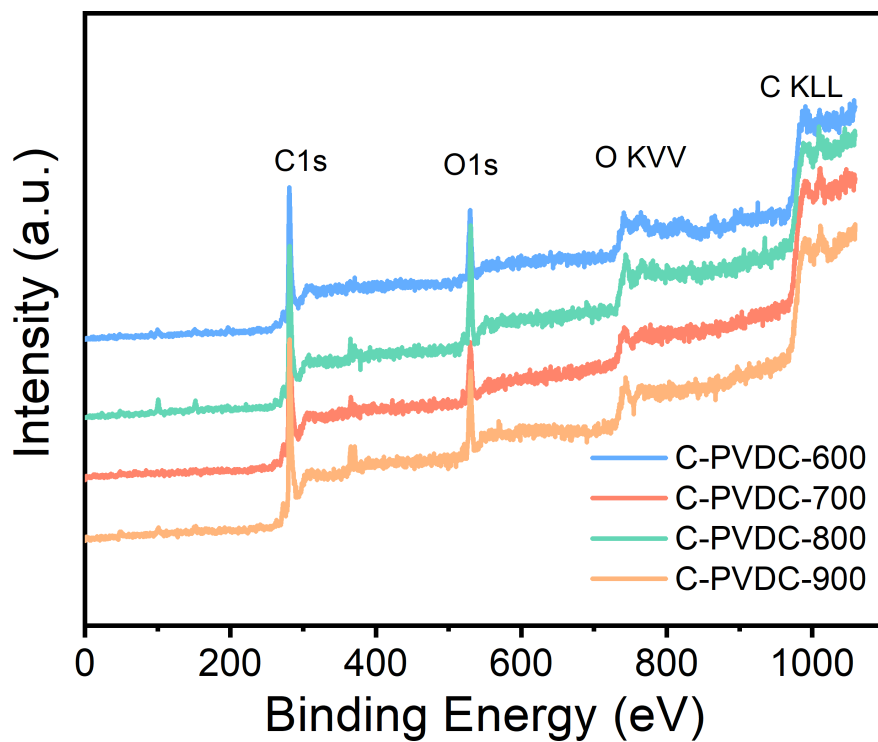
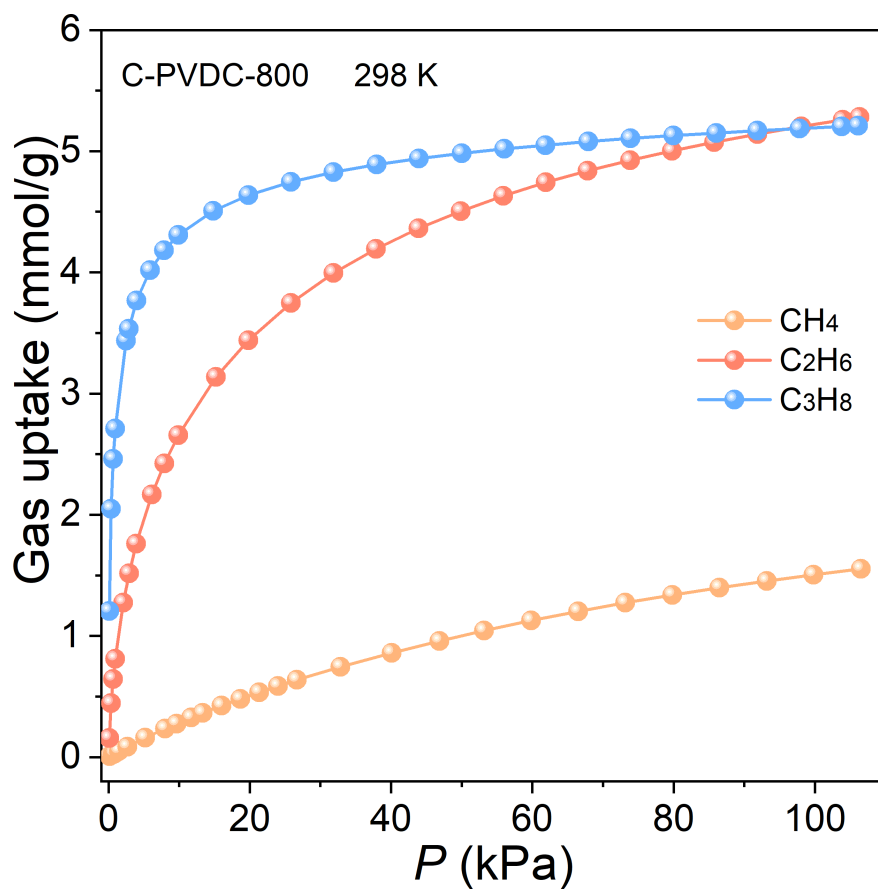
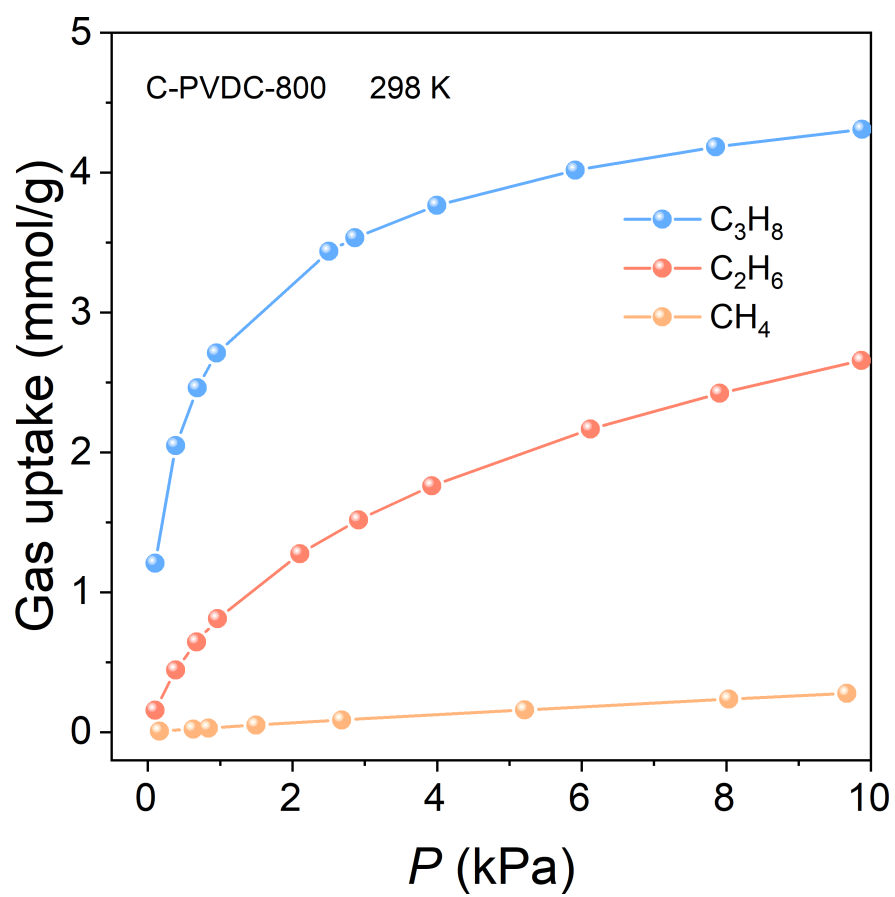
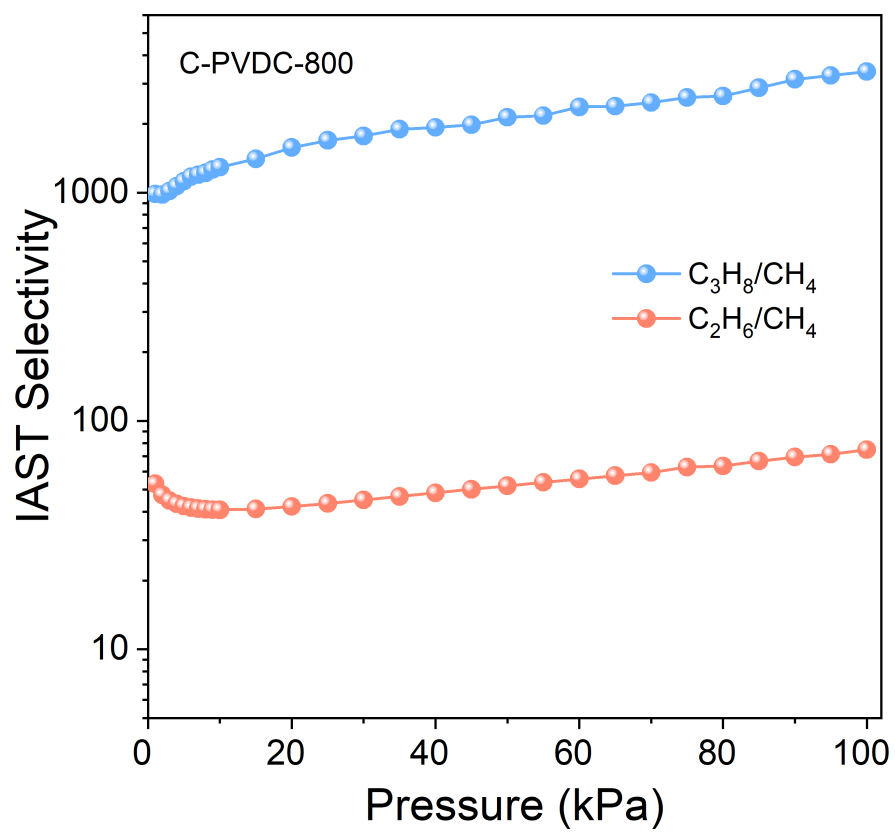
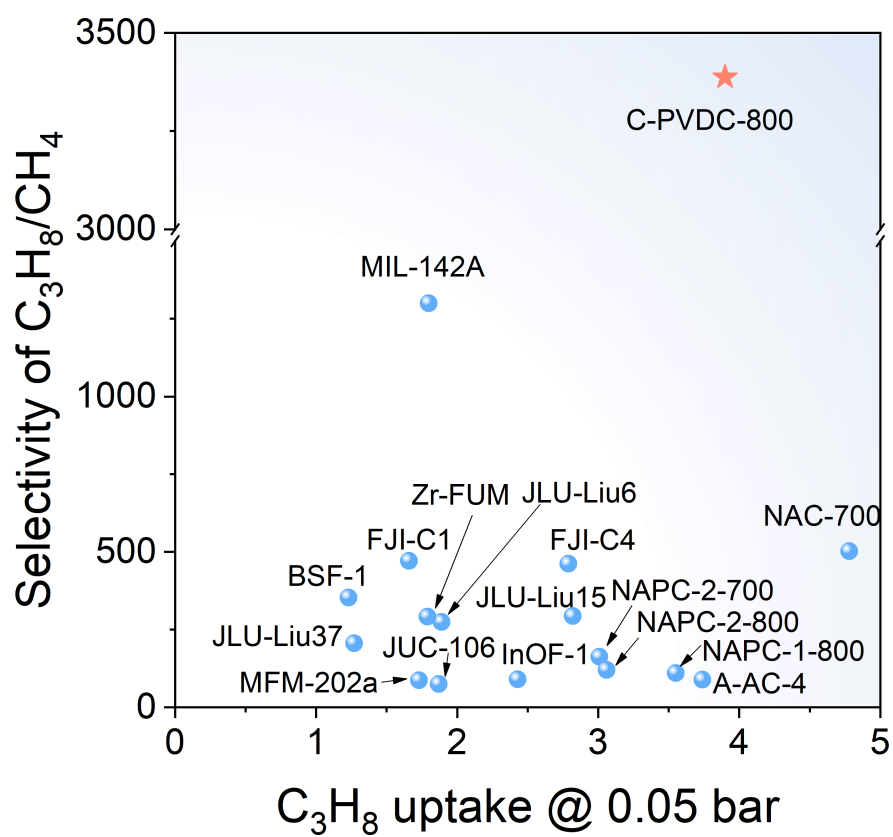


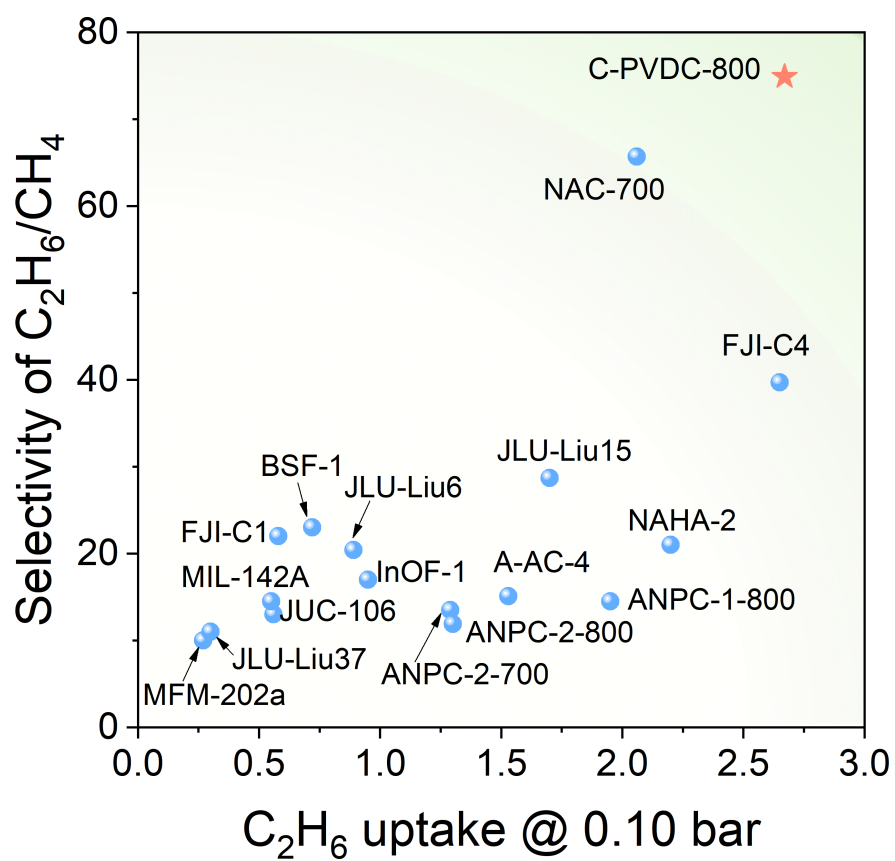
Fig. 1. (a) PXRD patterns of carbon adsorbents; (b) SEM image of C-PVDC-800; (c) Raman spectra of carbon adsorbents; (d) XPS spectra of carbon adsorbents.











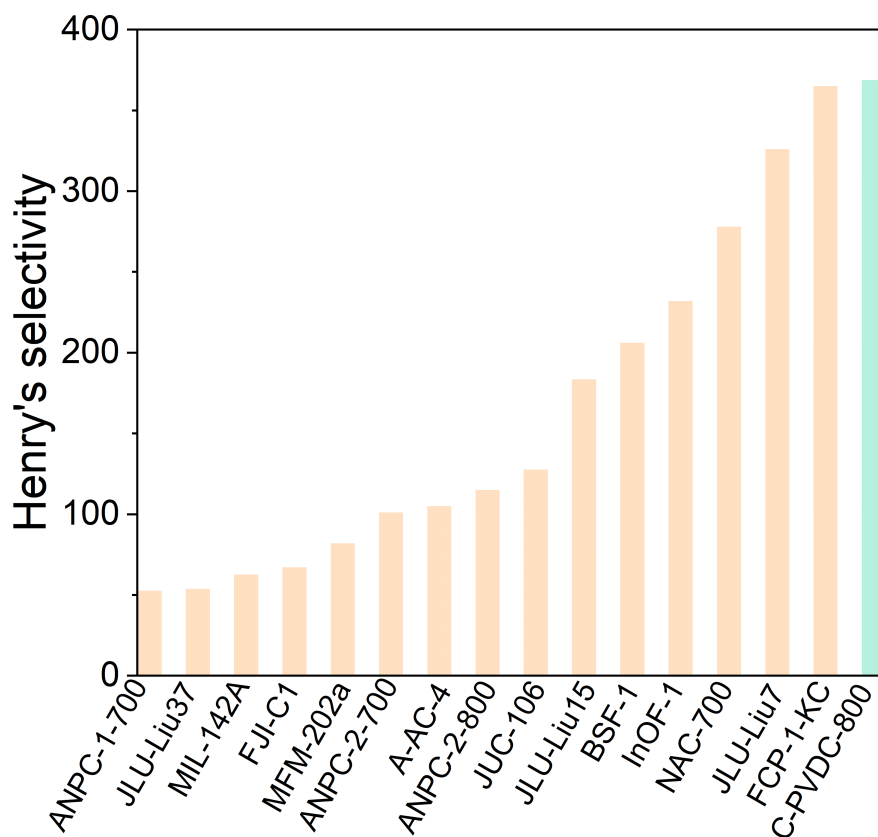
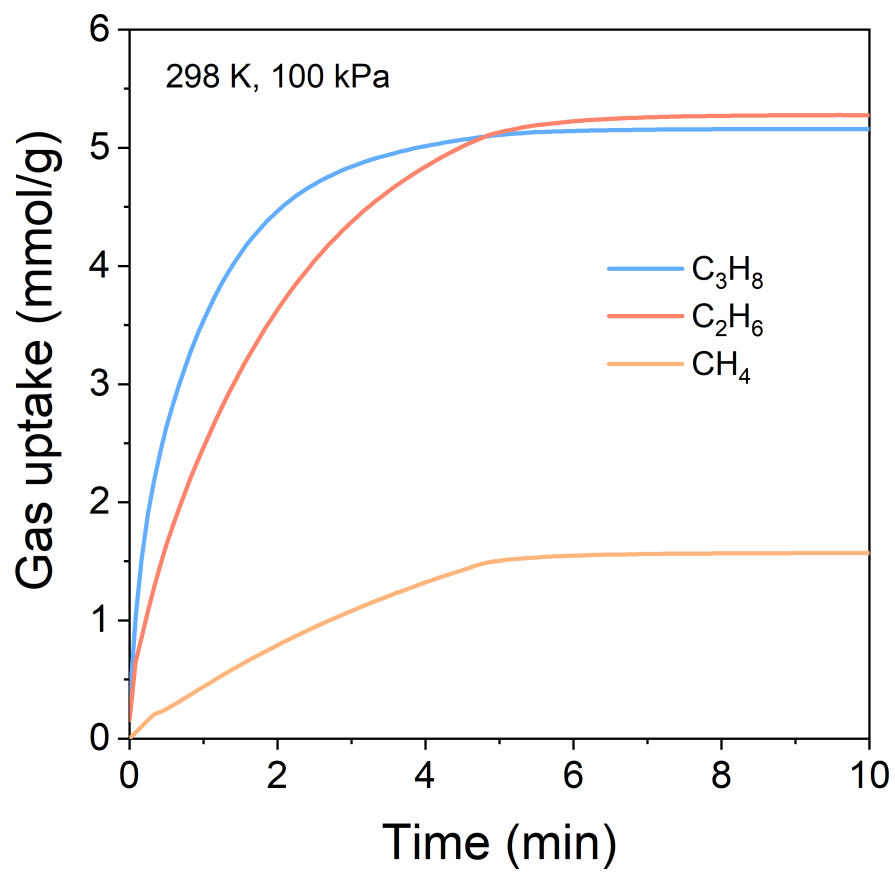
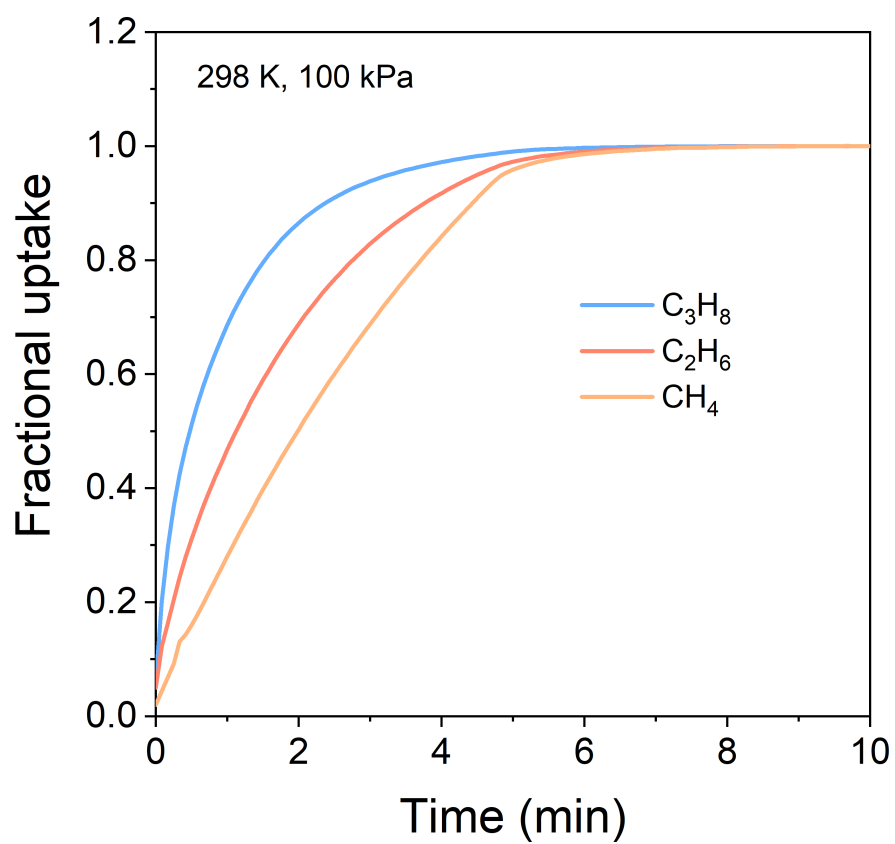


Fig. 2. Adsorption isotherms of C_3H_8 , C_2H_6 and CH_4 at 0-100 kPa (a) and 0-10 kPa (b) on C-PVDC-800 at 298 K; (c) IAST selectivity of C_3H_8/CH_4 (50/50, v/v) and C_2H_6/CH_4 (50/50, v/v) on C-PVDC-800 at 298 K; (d) Comparison of C_3H_8 uptake at 0.05 bar and IAST selectivity of C_3H_8/CH_4 (50/50, v/v) among reported adsorbents; (e) Comparison of C_2H_6 uptake at 0.10 bar and IAST selectivity of C_2H_6/CH_4 (50/50, v/v) among reported adsorbents; (f) Henry's selectivity of C_3H_8/CH_4 among reported adsorbents.





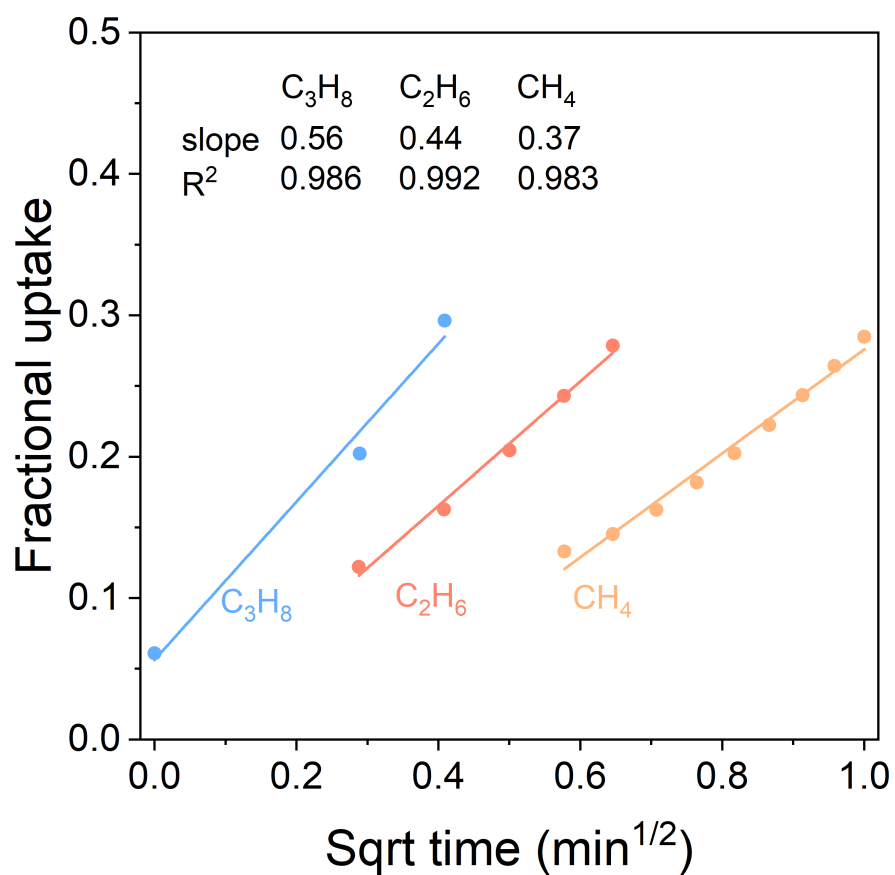
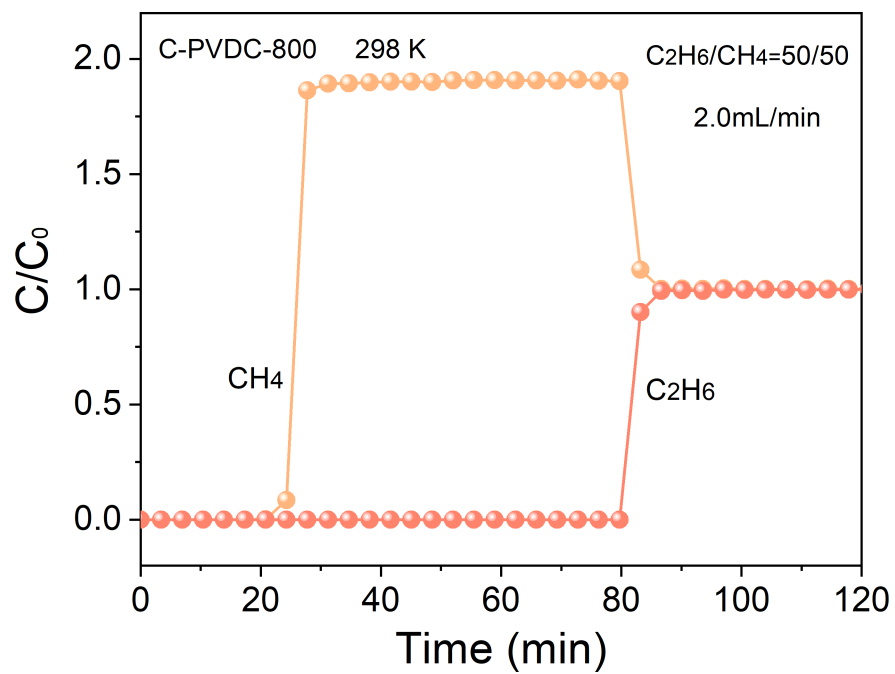
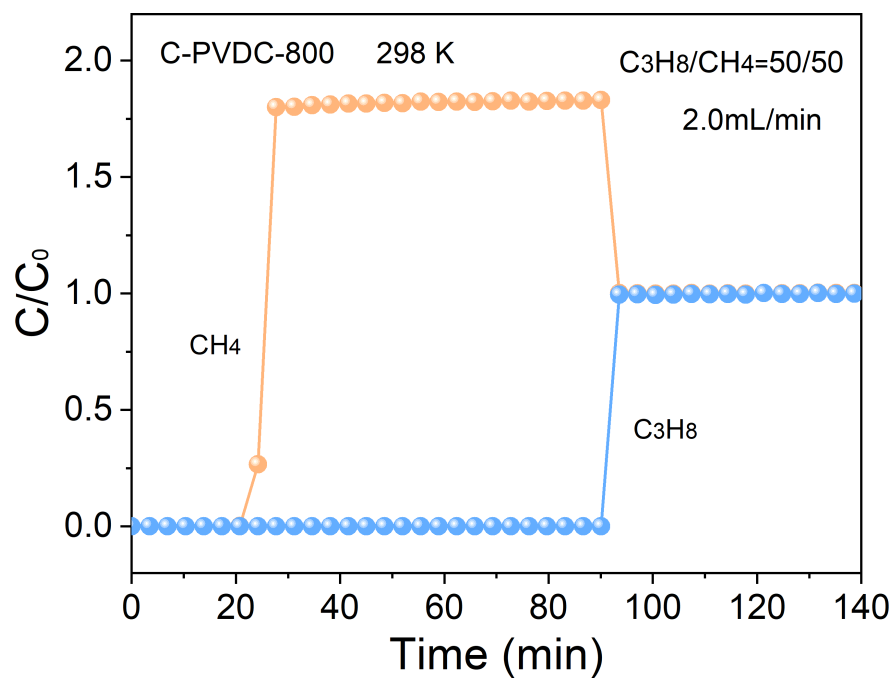


Fig. 3. (a, b) Time-dependant gas uptake profiles of C_3H_8 , C_2H_6 and CH_4 on C-PVDC-800 and fitting of diffusion time constants (c) at 100 kPa and 298 K.



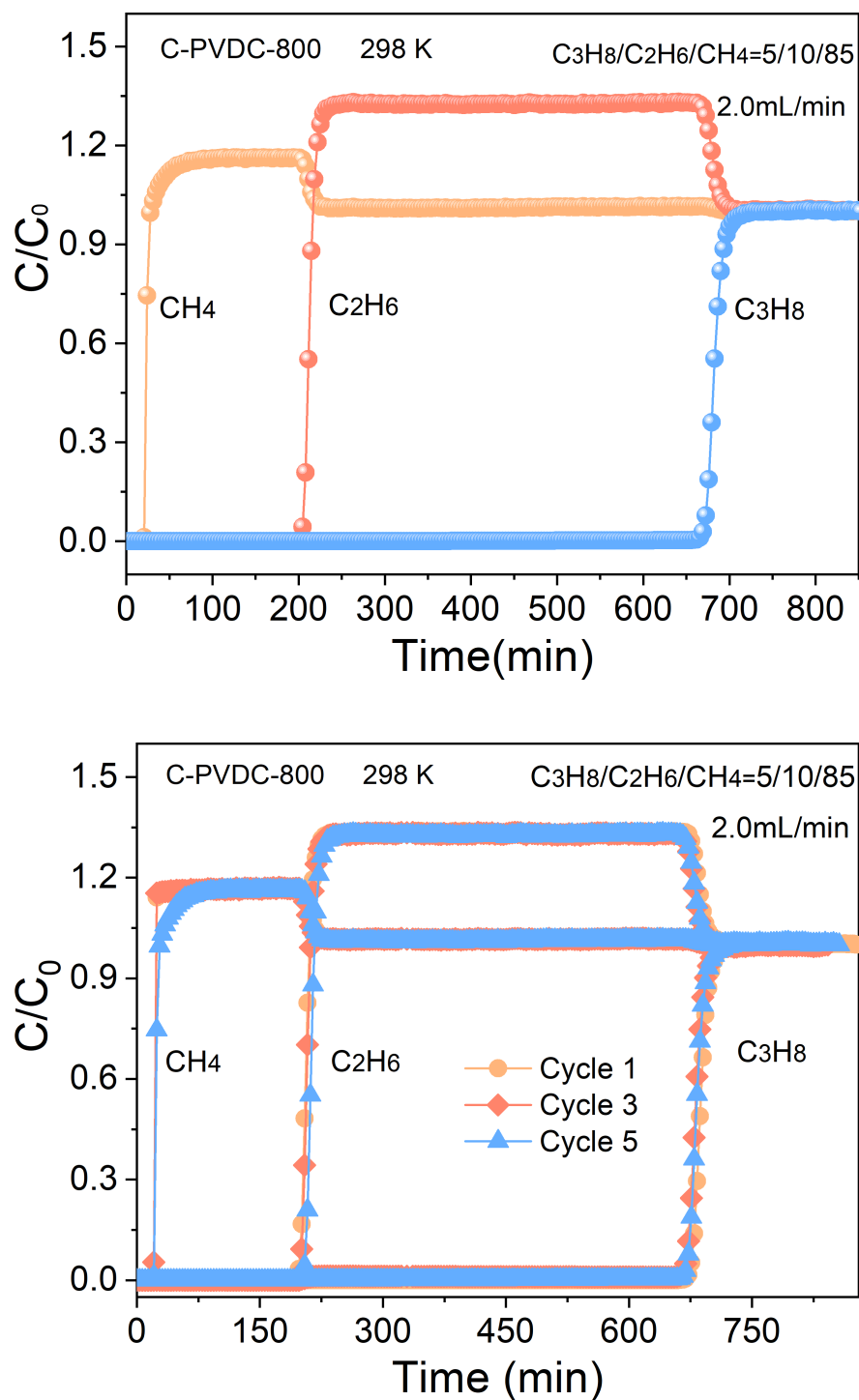


Fig. 4. Experimental breakthrough curves of (a) C_3H_8/CH_4 (50/50, v/v) and (b) C_2H_6/CH_4 (50/50, v/v) and (c) $C_3H_8/C_2H_6/CH_4$ (5/10/85, v/v/v) gas mixtures with a flow rate of 2.0 mL min⁻¹ on C-PVDC-800 at 100 kPa and 298 K; (d) Cycling breakthrough experimental curves of $C_3H_8/C_2H_6/CH_4$ (5/10/85, v/v/v) gas mixture on C-PVDC-800 at 100 kPa and 298 K. C_0 is the equilibrium concentration of outlet gas.

